European Journal of Cell Biology 53, 390-401 (1990) © Wissenschaftliche Verlagsgesellschaft mbH · Stuttgart

Immunocytochemical localization of glucocorticoid receptor in human gingival fibroblasts and evidence for a colocalization of glucocorticoid receptor with cytoplasmic microtubules

Gunnar Akner[1) a], Karl-Gösta Sundqvist[b], Marc Denis[a], Ann-Charlotte Wikström[a], Jan-Åke Gustafsson[a]

[a] Department of Medical Nutrition, Karolinska Institutet, Huddinge University Hospital, Novum F-60, Huddinge/Sweden
[b] Department of Clinical Immunology, Karolinska Institutet, Huddinge University Hospital, Novum F-60, Huddinge/Sweden

Received December 29, 1989
Accepted August 15, 1990

Fibroblasts — colocalization — glucocorticoid receptor — tubulin

The cellular distribution of the glucocorticoid receptor (GR) in relation to various intracellular and plasma membrane structures in human fibroblasts was studied using indirect immunofluorescence techniques with monoclonal and polyclonal antibodies. During interphase, GR was located predominantly in the cytoplasm, showing a similar pattern as tubulin. In mitotic cells, GR and tubulin were localized in mitotic spindles and in telophase midbodies. Colchicine and vinblastine induced a similar redistribution of GR and tubulin to the cell periphery. This redistribution was reversible for colchicine but not for vinblastine. Vinblastine also induced paracrystals containing GR and tubulin. These results support the hypothesis that GR interacts in vivo with cytoplasmic microtubules.

Introduction

The glucocorticoid receptor (GR) is an intracellular protein which, upon binding of a glucocorticoid hormone, interacts with specific DNA sequences involved in regulation of gene transcription [24, 48]. In cytosol prepared from cell homogenates, GR is found as a large M_r 300000 heteromeric aggregate. This complex contains, in addition to the M_r 94000 ligand and DNA-binding unit, a dimer of the heat-shock protein hsp90 [11, 13, 38] which represses the DNA-binding activity of the monomeric receptor protein in vitro [12]. A number of biochemical and immunocytochemical studies have supported the concept of a cytoplasmic localization of GR and its translocation to the nucleus in the presence of glucocorticoid hormones [1, 3, 17, 23, 36, 37, 41]. The apparent nuclear translocation occurs rapidly [37], and therefore random diffusion of cytoplasmic GR is quite unlikely, and instead a specific transport mechanism may be required.

There are indications that both GR and hsps may be linked to cytoskeletal components, i.e., GR to tubulin [45], hsp90 and hsp100 to actin [30, 31] and hsp90 to tubulin [40]. The present study was initiated in order to determine whether immunocytochemical evidence could be obtained for a colocalization of these proteins in the same cellular compartment(s). We therefore compared the cellular distribution of GR and various cytoskeletal proteins in interphase and mitotic cells under basal culture conditions, as well as after treatment of cells with microtubule (MT) inhibiting agents affecting the state of MT polymerization. The three major cytoskeletal networks were represented by actin (microfilaments), vimentin (intermediate filaments) and tubulin (MTs). Evidence is presented for a colocalization of GR with tubulin in normal human fibroblasts.

Materials and methods

Cells and media

Cultures of normal human fibroblasts (originally biopsy explants from the gingival mucosa) were subcultured as monolayers at weekly splits of 1:6 on ethanol-washed, heat-sterilized 18 × 18 mm glass coverslips (Chance Propper Ltd., Wapley/UK) in a moist atmosphere of 5% CO_2 and 95% air at +37 °C in 35-mm plastic culture dishes (Nunc, Roskilde/Denmark). The human fibroblasts were grown in a modified Eagle's minimum essential medium (MEM), i.e., complete Eagle's MEM including 28 μM phenol red supplemented with 2 mM L-glutamine, 60 mg/l (100000 IU/l) benzylpenicillin, 100 mg/l streptomycin sulfate and 10% (v/v) fetal bovine serum.

Manipulation of cell cultures

Cell cultures were treated for the indicated time periods by the following substances: colchicine 10 μM to 10 nM, demecolcine 10 μM, vinblastine 10 μM to 100 nM, cytochalasin B 100 to 10 μM.

[1)] Dr. Gunnar Akner, Department of Medical Nutrition, Karolinska Institutet, Huddinge University Hospital, Novum F-60, S-14186 Huddinge/Sweden.

Immunostaining procedure

Cell cultures were regularly stained on the second to fourth day of subculture. All incubations and washes were performed at room temperature except where otherwise mentioned. The whole staining procedure was carried out in sequence during the same day.

Initially, monostainings were performed. To study the distribution pattern of GR compared to that of cytoskeletal components, we used a double-staining, indirect immunofluorescence technique with fluorescein isothiocyanate (FITC) and Texas Red [42]. After having tested different fixation/permeabilization methods before the immunostaining, we found that the MT and microfilament networks were better preserved following methanol treatment compared to other procedures such as formaldehyde/Triton X-100. On the other hand, the preservation of GR, vimentin and nuclear antigens was the same regardless of the pretreatment method which was used. Thus, only methanol fixation was used in the present study. All antibodies were diluted in phosphate buffered saline (PBS) containing 0.1% (v/v) Triton X-100 and 3% (w/v) bovine serum albumin (BSA).

After fixation and all incubations, two washes were performed, the first in PBS containing 0.1% (v/v) Triton X-100, the other in PBS without detergent. After removing the culture medium, the cells were treated with methanol (−20 °C) for 10 min. After two washes for each 10 min, a mixture of the two first antibodies was added and incubated for 60 min. Following two 10-min washes, a mixture of the two second, fluorochrome-conjugated, antibodies was added and incubated for 45 min. After another two 10-min washes, the coverslips were mounted upside down on glass slides (Menzel Gläser, Braunschweig/FRG) in 50% (v/v) glycerol in PBS.

The immunofluorescence-stained cells were studied by a Nikon Labophot (Tokyo/Japan) immunofluorescence microscope equipped with epifluorescence optics using a 50× or 100× oil planapochromat objective, where excitation was obtained from a 100 W mercury lamp. FITC was visualized by using a Nikon B-2A excitation filter (450–490 nm) with an emission filter blocking reflected wavelengths of less than 520 nm. The corresponding filters used for visualizing Texas Red was a Nikon G-2A excitation filter (510–560 nm), emission filter blocking wavelengths of less than 590 nm. The excitation and emission spectra of these two fluorochromes have a low amount of overlap, and the fluorochromes can therefore be detected independently of one another on the same cell [42]. Microphotography was performed by a Nikon FX-35 A Data camera using Kodak Tri-X pan 400 ASA TX 135–36 black and white film exposing at an ASA setting of 800 for both FITC and Texas Red, adjusted to 0 for FITC and −2 for Texas Red, yielding exposure times of 7 to 20 s for FITC- and 2 to 6 s for Texas Red-labeled antigens. All pictures were taken using immersion oil (15577; Merck, Darmstadt/FRG).

Chemicals

Colchicine, demecolcine (=N-deacetyl-N-methyl-colchicine-colcemide), vinblastine sulfate and cytochalasin B were analytical grade products obtained from Sigma, St. Louis, MO/USA. Cell media and supplementary components were purchased from Gibco, Uxbridge, Middlesex/UK. Purified calf brain tubulin was a generous gift from Margareta Wallin, Department of Zoophysiology, University of Göteborg/Sweden.

Antibodies

The following primary antibodies were used:

Antibodies directed against intracellular antigens. 1) A monoclonal mouse anti-rat liver glucocorticoid receptor IgG 2a designated "mab 7" [35] in ascites, diluted 1:100, yielding a final protein concentration of 0.26 mg/ml. This antibody cross-reacts with the human GR [8]. *2)* A monoclonal mouse anti-chicken gizzard actin IgG 1 kappa (Biogenex Lab., Dublin, CA/USA), in ascites, diluted 1:100. *3)* A monoclonal mouse anti-porcine eye lens vimentin IgG 2a (Biogenex Lab.) in ascites, diluted 1:100. *4)* A polyclonal rabbit anti-sea urchin egg tubulin heterodimer (Dakopatts, Glostrup/Denmark) in serum, diluted 1:100, yielding a final protein concentration of 0.51 mg/ml. *5)* A pooled serum from patients with circulating antibodies directed against nuclear antigens, i.e., ANA-serum (Department of Clinical Immunology, Huddinge Hospital, Huddinge/Sweden), diluted 1:50.

Antibodies directed against plasma membrane antigens. 1) A monoclonal mouse anti-human Leu-3a IgG 1 (Becton Dickinson, Mountain View, CA/USA), diluted 1:100, yielding a final protein concentration of 0.25 µg/ml. *2)* A monoclonal mouse anti-human Leu-4 IgG 1 (Becton Dickinson), diluted 1:100, yielding a final protein concentration of 0.50 µg/ml. *3)* A monoclonal mouse anti-human transferrin receptor IgG 2a (Becton Dickinson), diluted 1:100, yielding a final protein concentration of 1.0 µg/ml.

The following secondary polyclonal antibodies were used: *1)* An FITC-conjugated goat anti-mouse Ig (Becton Dickinson), diluted 1:10, yielding a final protein concentration of 25 µg/ml. *2)* A Texas Red-conjugated donkey anti-rabbit Ig (Amersham International plc, Amersham/UK), diluted 1:25 yielding a final protein concentration of 20 µg/ml. *3)* An FITC-conjugated sheep anti-human Ig (National Bacteriological Lab., Stockholm/Sweden), diluted 1:50, yielding a final protein concentration of 0.27 mg/ml.

The buffer used for dilution, washes and substitute for primary or secondary antibodies as a negative control was PBS composed of 137 mM NaCl, 8 mM Na_2HPO_4, 3 mM KCl, 1.5 mM KH_2PO_4, *p*H 7.35.

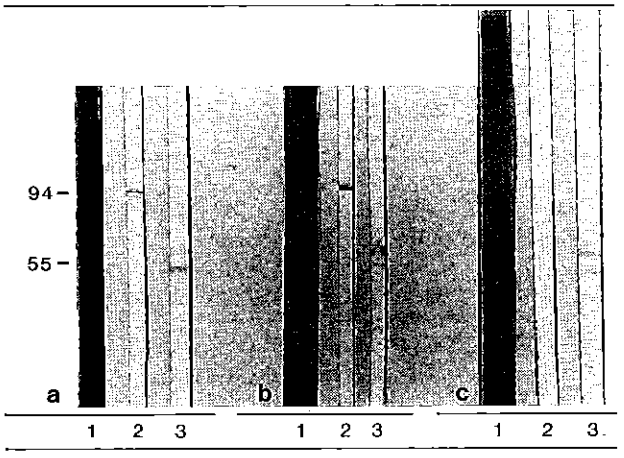

Fig. 1. Western immunoblotting showing rat liver cytosol (a), purified rat liver GR (b) and purified bovine brain tubulin containing 80% tubulin and 20% microtubule-associated proteins (MAPs) (c). Each sample is shown after Coomassie staining of the gel before electroblotting *(lanes 1)* and after electroblotting and probing the nitrocellulose filter with antibodies to GR *(lanes 2)* and tubulin *(lanes 3)*. Both antibodies recognized their own antigen without any cross-reactivity between the antibodies. The GR-antibody did not recognize any antigen in the purified tubulin fraction. The tubulin antibody recognized a double band around M_r 55000 in the purified GR-preparation indicating that purified GR also contains copurified tubulin immunoreactivity. Purified GR-preparations always contain proteolytic fragments, which may account for some of the lower M_r bands on the stained gel. The purified tubulin preparation contains besides tubulin around 20% MAPs, mostly HMW (high molecular weight MAPs); M_r around 300000. Molecular weight $\times 10^{-3}$ is indicated to the left.

Gel electrophoresis

The gel was a 60 × 90 × 0.75 mm sodium dodecyl sulfate-polyacrylamide (SDS-PAGE) vertical slab gel (stacking gel 3%, separating gel 9%, w/v) in a Bio-Rad Laboratories (Richmond, CA/USA), Mini-Protean II dual slab cell in a discontinuous buffer system under denaturing conditions as described by Laemmli [32].

Samples were: *a)* cytosol from rat liver prepared according to Denis et al. [11]. *b)* GR from rat liver, purified according to Wrange et al. [47]. *c)* A crude tubulin fraction containing 80% tubu-

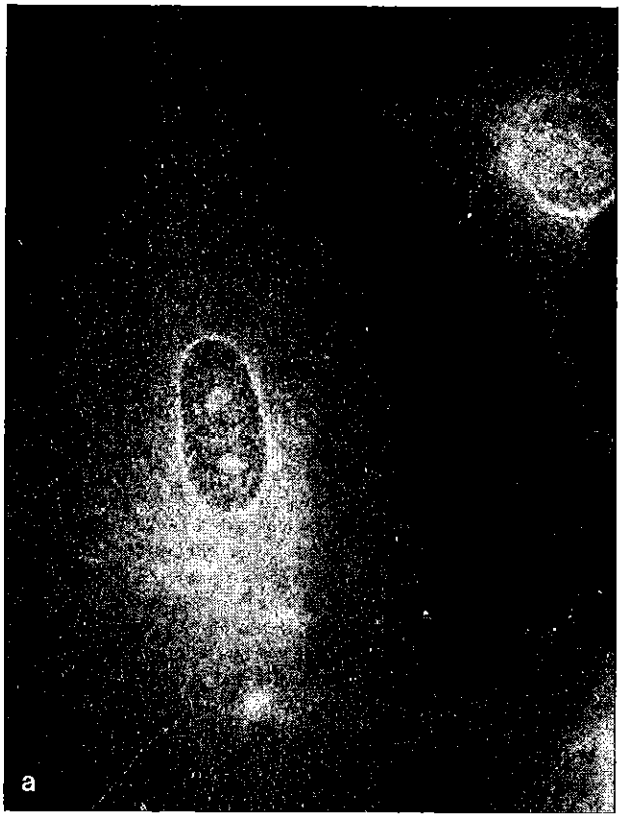

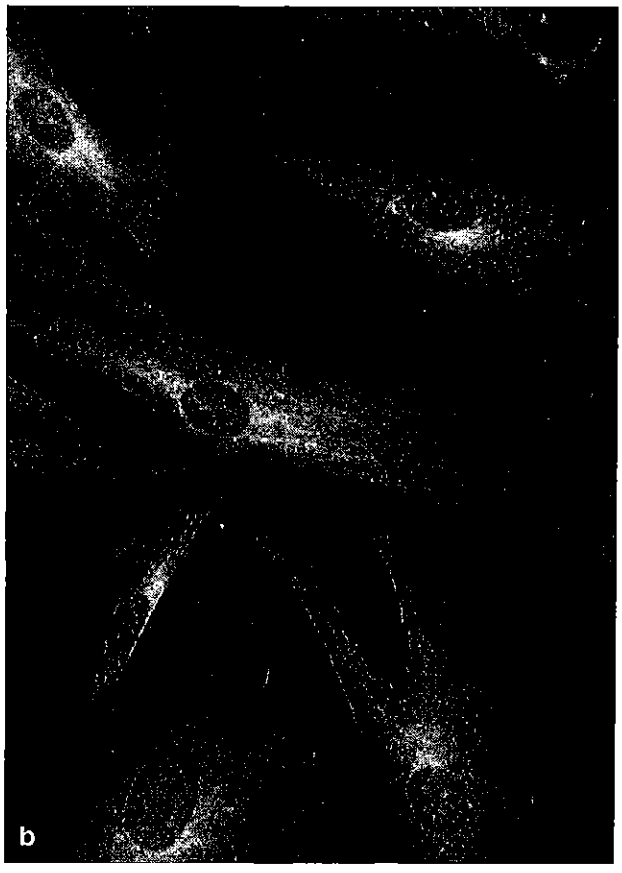

Fig. 2. Staining of interphase fibroblasts during basal culture conditions. — **a.** Monostaining of GR. — **b, c.** Double-staining of GR (b) and tubulin (c). — **d, e.** Double-staining of GR (d) and tubulin (e). — **f.** Monostaining of tubulin using Texas Red. — **g.** The same cell as in (**f**) using the FITC imaging system. — GR seems to be distributed along cytoplasmic microtubules *(arrows).* Parts of the leading edge of the ruffling membrane often exhibit more intense GR-staining *(arrowheads).* There is a very limited amount of overlap from Texas Red into the FITC imaging system. — 1310 × (a, d–g), 655 × (b, c).

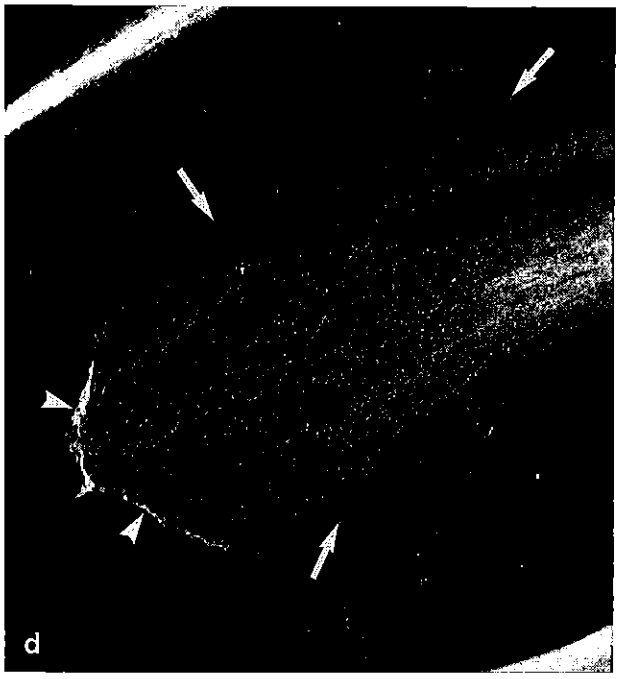

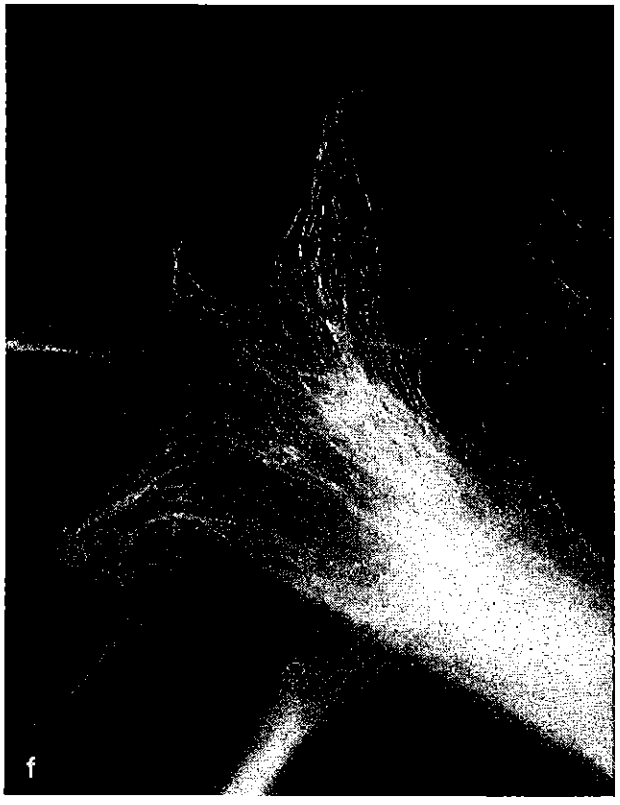

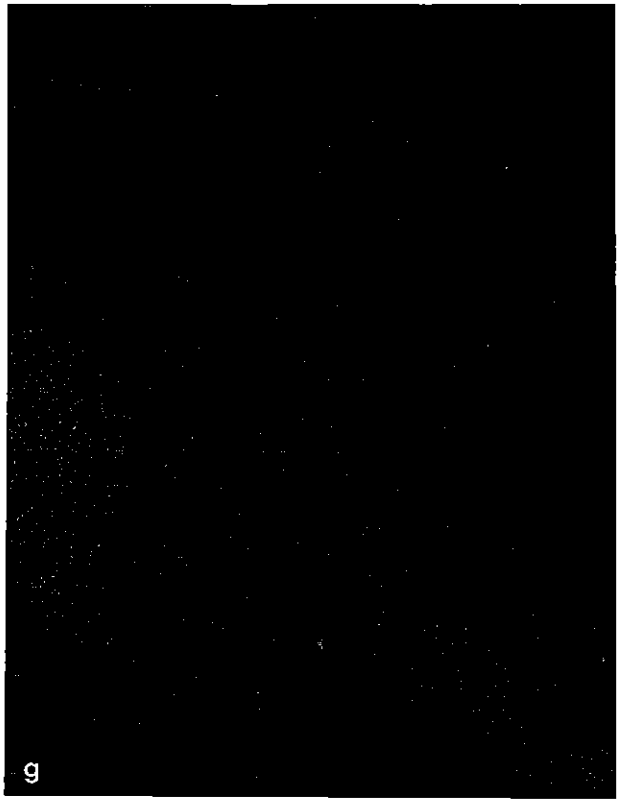

lin and 20% microtubule associated proteins (MAPs; purified according to Borisy et al. [5]).

Each sample was mixed with sample buffer containing 70 mM Tris-HCl, *p*H 6.8, 2% (w/v) SDS, 5.5% (v/v) 2-mercaptoethanol, 12.7% (v/v) glycerol and 0.001% (w/v) Bromophenol Blue, followed by heat denaturation at 100 °C for 2 min. Cytosolic proteins (15 µg), 1 µg GR and 8 µg tubulin were loaded to each SDS-PAGE well in a total volume of 20 to 30 µl of sample buffer. Electrophoresis was carried out by 200 V, constant voltage for usually 30 to 45 min in a running buffer containing 25 mM Tris, *p*H 8.3, 192 mM

glycine and 0.1% (w/v) SDS. The calibration kit was MW-SDS-200-kit from Sigma. Protein concentration was determined according to the method of Bradford [6] using BSA as standard. After electrophoresis, gels were stained with 0.15% Coomassie Brilliant Blue in 50% methanol and 10% acetic acid for 1 h and destained with 25% methanol and 10% acetic acid.

Western immunoblotting

Proteins were transferred from the SDS-PAGE gel to a nitrocellulose (NC) membrane (M-filter, BA83, pore size 0.2 μm, Schleicher and Schuell, Dassel/FRG) by electroblotting at 200 mA, constant current, for 1 h in an LKB (Bromma/Sweden) Midget Multiblot electrophoretic transfer unit using a transfer buffer containing 25 mM Tris, 192 mM glycine and 20% (v/v) methanol, *p*H 8.6 at +4 °C. The efficiency of electroblotting was checked by Coomassie staining of gels after blotting. Strips of the NC-filter were cut by a scalpel. Nonspecific binding was blocked by incubation with 3% (w/v) defatted dry milk in PBS overnight, and the filter was then directly transferred to the first antibody solution. All antibodies were diluted in PBS containing 0.05% (v/v) Tween-20 and 1% (w/v) defatted milk. Three washes of each 10 min were performed in PBS, PBS-0.05% (v/v) Tween 20 and PBS, respectively. The first antibody was incubated for 1 to 2 h at room temperature. As a second antibody, we used a horseradish peroxidase (HRP)-labeled goat anti-mouse/rabbit IgG (Bio-Rad) diluted 1:800. The immunostaining was developed by using an HRP-color development solution (Bio-Rad) containing 60 mg 4 α-chloro-1-naphthol dissolved into 20 ml −20 °C methanol and immediately before usage mixed with 100 ml PBS containing H_2O_2, yielding a final H_2O_2 concentration of 0.015%. The staining was developed for 5 to 30 min followed by two 10-min washes in distilled water and air-drying.

Ligand binding experiments

Glucocorticoid binding in fibroblasts was determined by a modification of a whole cell binding technique described by Gadson et al. [18]. Normal human gingival fibroblasts were grown to confluence in 35-mm plastic culture dishes (Nunc). The medium was evacuated and replaced by fresh medium containing 1, 2, 5, 10, 25, and 50 nM [^{3}H]dexamethasone in the presence or absence of a 200-fold excess of the same, unlabeled glucocorticoid. Dishes were incubated for 4 h in triplicate for each concentration of glucocorticoid. Some dishes were treated with colchicine or vinblastine, both at 10 μM, for 1 h followed by only dexamethasone for 4 h, at the indicated concentrations. Following the glucocorticoid incubation, the dishes were placed on ice and washed with cold PBS until no radiolabeled material could be detected in the wash (usually three washes); the low temperature was in order to minimize dissociation of glucocorticoid from its receptor. The monolayers were allowed to dry, solubilized with 0.75 ml 0.2% (w/v) SDS, and 0.25-ml aliquots in duplicates were transferred to counting vials containing 4 ml scintillation emulsifier (Beckman Ready Safe; Beckman, Instruments, Inc., Fullerton, CA/USA). Radioactivity was measured in a 1216 Rackbeta II liquid scintillation counter (LKB-Wallac) at 30% efficiency for tritium.

Specific binding was calculated by subtracting disintegrations per minute (dpm) in nonspecific dishes from those dishes to which no competitor was added and then subjected to Scatchard analysis. Parallel dishes with confluent fibroblasts in triplicate after standard trypsinization (21 μM trypsin and 0.54 mM EDTA) were counted. The specific activity of [^{3}H]dexamethasone was 44.7 Ci/mmol, and 1 pmol of [^{3}H]dexamethasone corresponded to 90000 dpm. The number of binding sites per fibroblast were calculated assuming a molecular weight of 94000 for GR and 1:1 ratio of ligand to receptor.

Results

Specificity control

The monoclonal antibody mab 7, raised against rat liver GR [35] has previously been shown to monospecifically react with GR in crude rat liver cytosol by Western blotting technique [35]. By a whole cell competitive ligand binding assay using 1 to 50 nM dexamethasone, the human gingival fibroblasts were found to contain around 110000 specific glucocorticoid binding sites per cell. Induction of MT-depolymerization by colchicine or vinblastine induced a reduction in GR-binding sites to 100000 and 90000 sites per cell, respectively. The dissociation constant (Kd) was between 4 to 5 nM regardless if the cells were pretreated with colchicine/vinblastine or not.

Western immunoblotting performed on purified GR and purified tubulin revealed that the antibodies used against GR and tubulin recognized their own specific antigen without cross-reacting with any of the other antigens (Fig. 1). The GR-antibody did not recognize any antigen in the purified tubulin fraction. The tubulin antibody recognized a double band around M_r 55000 in the GR-preparation, indicating that purified GR also contains tubulin immunoreactivity. Control stainings using monoclonal antibodies against human lymphocyte plasma membrane structures like Leu-3a, Leu-4 and the transferrin receptor (not shown) were always negative, as were all controls where PBS substituted for either the first or the second antibody. The amount of overlap between the fluorophores were minimal (cf. Figs. 2f and g).

Preblocking the anti-GR-antibody with excess of purified calf brain tubulin did not significantly reduce the GR-fluorescence intensity (not shown). All incubations and 50% of the washes (for immunostainings and immunoblottings) contained high concentration of detergent, which reduces nonspecific antigen-antibody reactions.

Preincubation with nonimmune serum from the animal species in which the second antibody was raised did not affect the staining, and this step was therefore omitted.

Immunostaining of interphase cells during basal culture conditions

The typical GR-staining of normal human fibroblasts is shown in Figures 2a, b and d. The GR was found predominantly in the cytoplasm but also in the nucleus. The most intense staining was in the perinuclear area. The fibrillary staining pattern of the cytoplasm extended into the lamel-

Fig. 3. Double-staining of mitotic cells during basal culture conditions. — **a, b.** GR (**a**) and tubulin (**b**). — **c, d.** GR (**c**) and tubulin (**d**). — **e, f.** Vimentin (**e**) and tubulin (**f**). — GR is colocalized with tubulin in mitotic spindles and telophase midbodies *(arrows)*. GR is also localized along the cell periphery in mitotic cells *(arrowheads)*. Vimentin is not localized within mitotic spindles or midbodies. — 1310× (**a, b**), 655× (**c–f**).

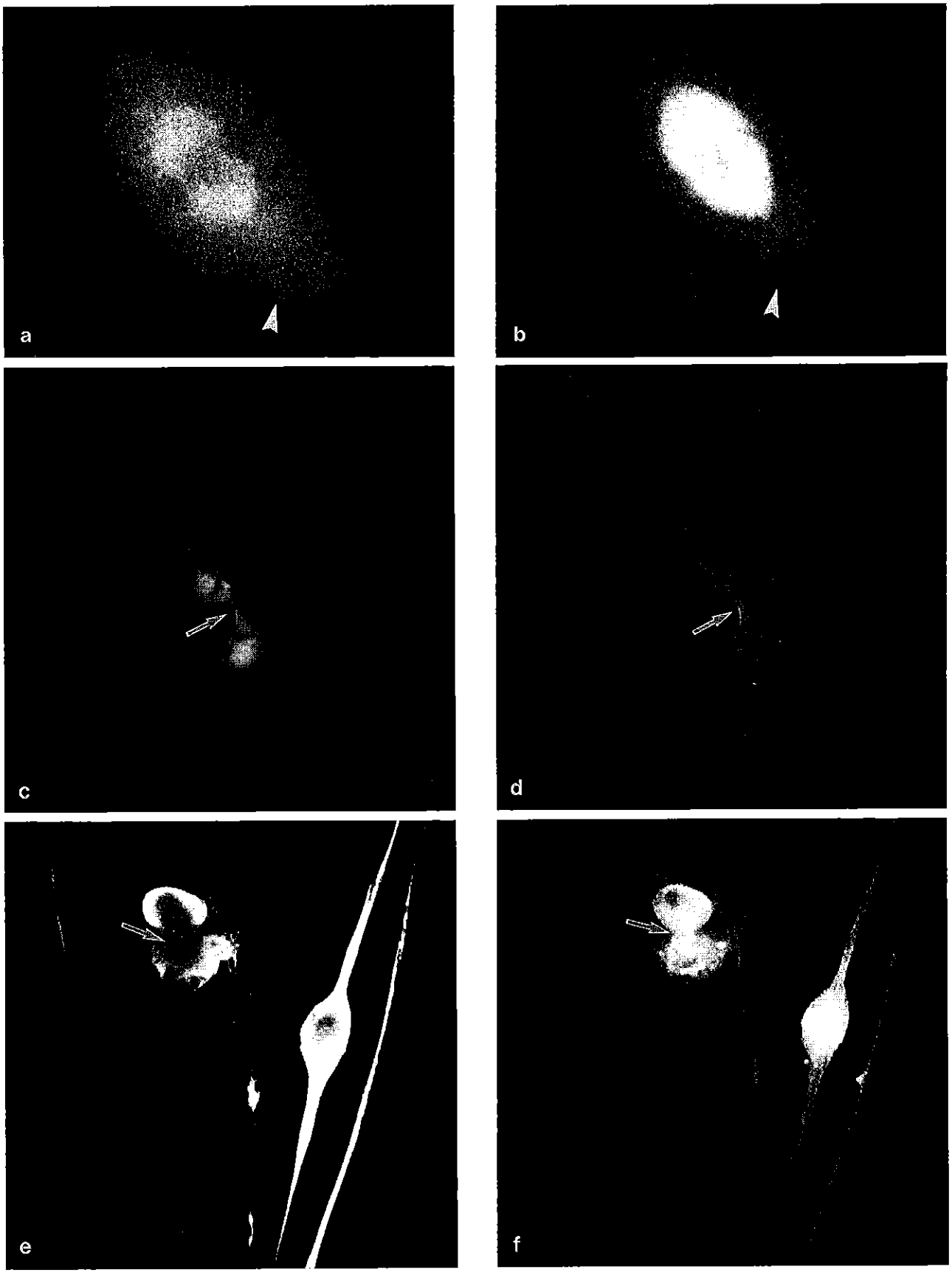
a
b
c
d
e
f

lipodium, with the fibrils travelling essentially parallel to the long axis of the cell. Parts of the leading edge of the ruffling membrane were usually more intensely stained, while the rest of the plasma membrane remained negative (Fig. 2d). The nucleus exhibited a weak but distinct, irregular pattern. There was always an intensely stained narrow zone at the nuclear periphery. Experiments using confocal laser microscopy producing 1 μm thick optical sections of stained human fibroblasts revealed that this nuclear staining was not due to a projectional artifact from cytoplasm surrounding the nucleus (results to be published elsewhere). Our finding of GR-staining in both the cytoplasm and the nucleus under basal cell-culture conditions was also strengthened by the observation of similar staining of both of these compartments in cryostat sections of pelleted and formaldehyde-fixed fibroblasts where many nuclei had been cut open by the cryostat without any chemical permeabilization (not shown).

Tubulin (Figs. 2c, e, f), actin (not shown), and vimentin (not shown) all exhibited typical staining patterns previously described [25, 33, 43]. The distribution pattern of vimentin was somewhat similar to those of GR and tubulin, however, the size and course of the vimentin fibers were different; they were more curved, and they usually ended more closely to the nucleus than GR and tubulin, leaving a clear zone in the peripheral part of the lamellipodium. The pooled patient serum containing anti-nuclear antibodies gave rise to an intense staining in all parts of the nuclei (not shown). The cytoplasm and the plasma membrane remained negative.

In double-staining experiments, the cytoplasmic, fibrillary distribution of GR was similar to that of tubulin (cf. Figs. 2b and c; 2d and e). The fibrillar pattern of vimentin showed some similarities with GR at the center of the cell but was different from GR towards the periphery of the lamellipodia (not shown). The GR-staining was different from those of actin (not shown) and nuclear antigens (not shown).

Immunostainings of mitotic cells during basal culture conditions

The general staining intensity of GR in mitotic fibroblasts was higher than in the surrounding interphase cells (Fig. 3a). GR exhibited intense staining of the pericentriolar regions and the mitotic spindles (Fig. 3a) in mitotic cells with a clear zone in the middle corresponding to the equator. During the mitotic separation, the GR-immunoreactivity followed the migration of the spindle structure towards the opposite poles of the cell (not shown). The intercellular bridges (midbodies) in late mitotic telophase, known to contain tightly packed MTs, also exhibited GR-immunoreactivity (cf. Figs. 3c and d). In addition, mitotic cells often had several processes around their circumference containing strong GR-staining (not shown). These findings were confirmed by staining various fast growing cell lines exhibiting more abundant mitotic cells, i.e., a rat Reuber hepatoma cell line denoted H-4-II-E, HeLa cells, and a human mesothelioma cell line established in our laboratory. As expected, tubulin was localized both in the pericentriolar areas, mitotic spindles (Fig. 3b) and in postmitotic midbodies (Fig. 3d). Vimentin (Fig. 3e) was distributed along the plasma membrane in mitotic cells in a similar fashion as actin (not shown). Vimentin was not seen within mitotic spindles or in midbodies; neither was this the case for actin (not shown). Double-staining experiments showed colocalization of GR and tubulin during mitosis (cf. Figs. 3a and b; 3c and d).

Effect of microtubule inhibitors on the immunostainings

After 20 to 30 min of treatment with either colchicine or demecolcine, the fibroblasts started to project pseudopods and microspikes [4], while the general cell shape became more rounded. The cells were exposed to these agents at a concentration of 10 μM to 10 nM for 60 to 120 min and were then processed for immunocytochemistry. Double-staining experiments showed that GR and tubulin immunoreactivities were distinctly and similarly redistributed within the cell after both colchicine and demecolcine treatment (cf. Figs. 4a and b). The perinuclear GR-zone was smaller, and the cell surface projections contained intense GR-staining (Fig. 4a). There was usually a relatively large negative zone between the perinuclear area and the stained processes. The nuclear staining remained unchanged. The number of visible mitoses was not increased. A dose response analysis revealed that these changes occurred most markedly at a concentration of 10 to 1 μM, while being less evident at 100 nM colchicine.

Staining for tubulin showed that the MT network had now disappeared (Fig. 4b). Instead, there was a diffuse, nonfibrillar zone around the nonstained nucleus, and both types of processes were also well stained for tubulin. Double-staining for actin and tubulin (cf. Figs. 4c and d) after colchicine treatment showed the actin pattern to be unaffected, with no signs of peripheral redistribution within the cell, while tubulin was redistributed to the cell periphery similarly to GR. Vimentin was affected by colchicine treatment in a different way than GR and tubulin; the vimentin pattern was condensed to a small area around the nucleus without any staining in the cell surface projections (not shown). All morphological changes induced by treatment with colchicine for 1 h were reversible after changing to normal culture medium overnight.

Vinblastine is known to induce depolymerization of MT and formation of crystalline inclusion bodies also known as paracrystals [16]. Vinblastine induced less rounding up of the cells than colchicine/demecolcine. The kinetics for induction of cell processes was, however, essentially the same. The cells were exposed to vinblastine at 10 μM to 100 nM for 60 to 120 min and then processed for immunocytochemistry.

The GR-staining remained mainly in the perinuclear area, but there was also a peripheral redistribution into the two different types of processes with a negative zone in between, as seen for colchicine/demecolcine. The nuclear staining was unchanged. However, we also observed that all the cells contained large amounts (10–100 per cell) of strongly GR-stained, regular, rectangular paracrystals of different size (Fig. 5a).

Staining for tubulin (Figs. 5b, d) showed a complete breakdown of the MT fibrillary system including the dif-

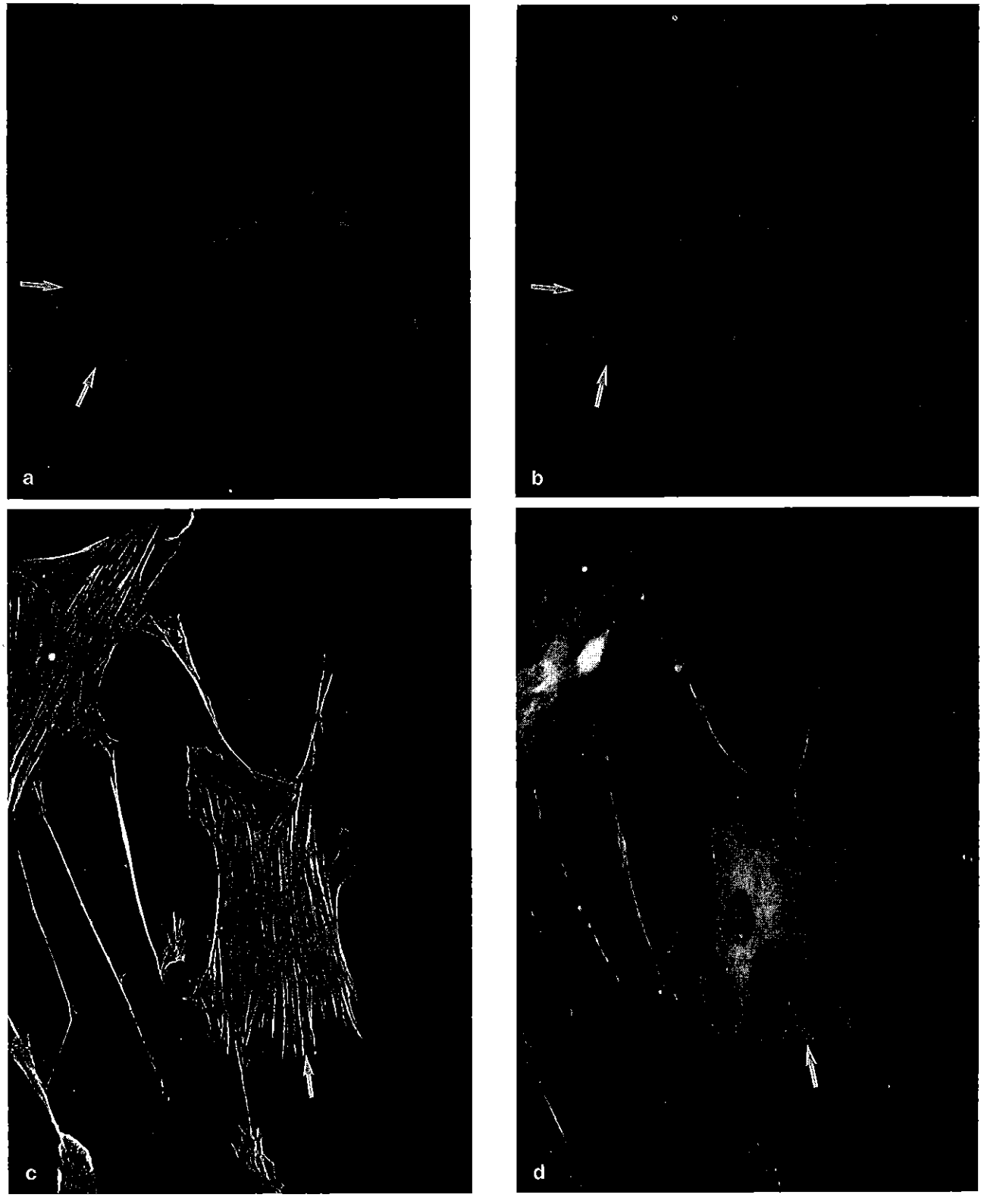

Fig. 4. Double-staining of fibroblasts after treatment with 10 μM colchicine for 1 h. — **a, b.** GR (**a**) and tubulin (**b**). — **c, d.** Actin (**c**) and tubulin (**d**). — GR is redistributed to processes in the cell periphery *(arrows)* where it is colocalized with tubulin but not with actin. — 655 ×.

fuse perinuclear staining that was still seen after colchicine treatment. All cells exhibited tubulin staining localized within the paracrystals and in the cell periphery (Figs. 5b, d).

Thus, most paracrystals were stained for both GR and tubulin. Also after vinblastine treatment, the redistributed GR correlated closely to tubulin at the cell periphery as when cells were treated with colchicine/demecolcine. Staining for vimentin (Fig. 5c) as compared to tubulin (Fig. 5d) did not show any sign of redistribution of vimentin to peripheral projections or to paracrystals. The distribution of actin (not shown) and nuclear antigens (not shown) was also unaffected after vinblastine treatment. The paracrystals were stained positive for GR as for tubulin also when monoimmunofluorescence staining was used, thereby eliminating the possibility of overlap between the two fluorochromes.

The vinblastine-induced morphological changes were only partly reversible after overnight culture in normal medium. Thus, the paracrystals disappeared, but the peripheral redistribution of GR and tubulin remained the same, thus the presence of vinblastine is probably necessary for both induction and maintenance of the paracrystals. The formation of paracrystals was only seen at vinblastine concentrations of 10 μM. At 1 μM to 100 nM, only peripheral redistribution was seen with a similar pattern for both GR and tubulin (not shown).

Effect of microfilament inhibitor on the immunostainings

Cytochalasin B is known to totally depolymerize microfilaments and to induce an arborization of the cell morphology [21]. Treating the fibroblasts with cytochalasin B at 100 to 10 μM for 1 to 24 h induced a typical arborization pattern exhibiting a totally disintegrated microfilament network (not shown). Double staining for GR and tubulin showed similar distribution of strong immunoreactivity towards the center of the cells extending into the various projections. The fibrillar networks were now less evident but showed very similar patterns for GR and tubulin and different from actin.

Discussion

Fibroblasts are target cells for glucocorticoid action [2, 7, 18, 34]. Usually skin fibroblasts have been studied. In this investigation we used normal, human, gingival fibroblasts and found around 110000 GR molecules per cell. The GR-binding capacity was reduced 10 to 20% without affecting the dissociation constant (Kd) after induced MT-depolymerization and concomitant GR-redistribution.

We studied the light microscopic intracellular distribution of GR in interphase and mitotic fibroblasts before and after induced depolymerization of cytoplasmic microtubules (MTs) and microfilaments. In interphase human fibroblasts, we observed a very similar distribution of GR and cytoplasmic MTs. The GR-pattern differed clearly from that of microfilaments (actin), but usually there was some resemblance with the pattern of the intermediate filament vimentin, especially towards the center of the cells. It is known that MTs and intermediate filaments can exhibit very similar fibrillar patterns in interphase cells [44, 46]. However, as discussed above and previously described by several authors [44, 46], there are also distinct differences in distribution of MTs and intermediate filaments, both in interphase and especially in mitotic cells and after treatment with MT-depolymerizing agents. The possibility exists that during interphase GR is colocalized with both MTs and intermediate filaments, at least in some parts of the cell, but because of the close similarities between GR and tubulin described in this study, we draw the conclusion that the GR-pattern corresponds best with that of cytoplasmic MTs. Treatment of the cells with tubulin depolymerizing drugs only affected GR and tubulin staining patterns, but did not alter the distribution of actin, vimentin or nuclear antigens, which supports the specificity of the GR-tubulin interaction.

During the cell cycle, tubulin of the cytoplasmic MTs is known to be recycled into the mitotic spindle, and the data presented here indicate that part of the cellular GR-content follows tubulin during the cell cycle.

The MT-inhibitors used in the present study are known to shift the dynamic equilibrium from the polymeric state (i.e., the intact MTs) in favour of a soluble subunit pool by binding to tubulin subunits and inhibiting polymerization. The net effect will therefore be a depolymerization of MTs [15]. Another MT-inhibitor, nocodazole, induced a similar redistribution of MTs in hamster fibroblasts [10]; the disassembly of the MTs proceeded predominantly from the center of the cell towards its periphery and produced an MT-depleted zone between the nucleus and the periphery.

Colchicine and vinblastine induced formation of two types of processes at the cell surface. The pseudopods are known from electron microscopic analysis to contain organelles like membranes of the rough endoplasmic reticulum, mitochondria and lysosomes, whereas the much smaller microspikes were found to contain only longitudinally oriented microfilaments [4]. From the results presented here, it is evident that both processes also contain GR and tubulin, but neither actin nor vimentin. Depolymerization of MTs induced a peripheral redistribution of GR indicating that MTs might be responsible for maintaining the position of GR in normal, interphase fibroblasts.

The ability of vinblastine to induce formation of paracrystals has been described previously [16]. The crystals are usually rectangular in shape, their long axis being up to 20 μm in length. Electron microscopic studies of cross-sectioned crystals have shown that they contain bundles of tightly packed MTs arranged in a hexagonal pattern of slightly enlarged MTs designated "macrotubules" (diameter around 32 μm), where one MT is surrounded by six others [16]. The walls of these "macrotubules" have a different structure compared to that of regular MTs. Variable amounts of the GR-staining remained in the perinuclear

Fig. 5. Double-staining of fibroblasts after treatment with 10 μM vinblastine for 1 h. — **a, b.** GR (**a**) and tubulin (**b**). — **c, d.** Vimentin (**c**) and tubulin (**d**). — GR is redistributed to numerous paracrystals where it is colocalized with tubulin but not with vimentin *(arrows)*. — 655×.

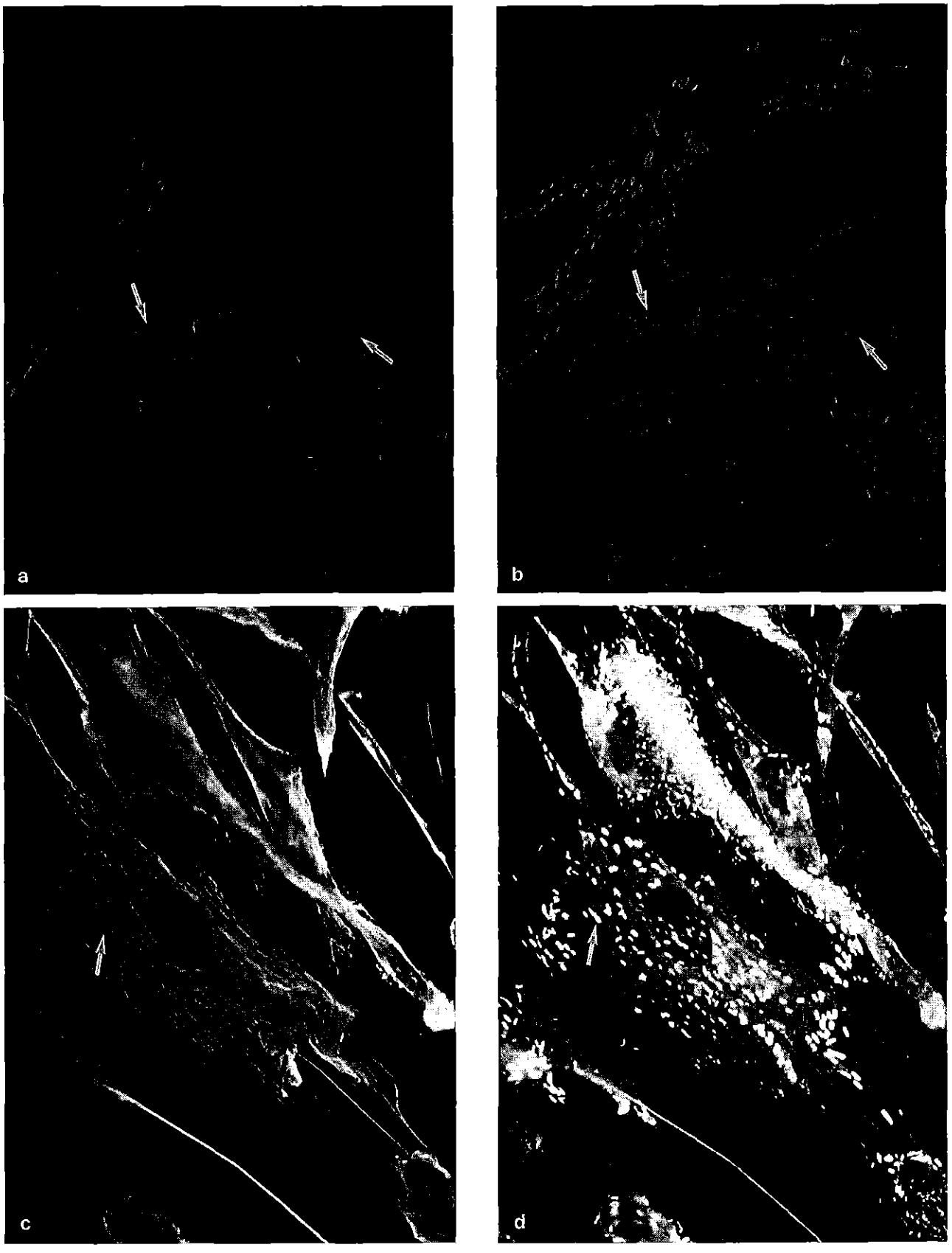
a
b
c
d

region after vinblastine treatment, possibly because only a smaller pool of GR was redistributed. After treatment of the cells with colchicine/demecolcine which induced complete disappearance of the MT fibrillary network, the anti-tubulin antibody still detected tubulin immunoreactivity, but now as a more diffuse staining, indicating that this antibody recognizes tubulin in both its polymerized and depolymerized state.

Cytochalasin B inhibits polymerization of G-actin into F-actin by binding to actin filaments and thus prevents addition of actin monomers [21]. In similarity to the mechanism of MT-depolymerization, this leads to a net effect of depolymerization of microfilaments. We observed that treating cells with cytochalasin B induced an accumulation of GR and tubulin towards the center of the arborized cell, again indicating an interaction between these molecules.

Very few reports deal with a possible interaction between GR and different cytoskeletal proteins. We have previously reported [45] a fibrillary, cytoplasmic staining of GR in a cell line derived from human hyperplastic cervix tissue (NHIK 3025). Indications of GR-tubulin interaction have also recently been found by Pratt and coworkers [39].

In preliminary experiments we have found that both immunoaffinity-purified and DNA-cellulose chromatography-purified (Fig. 1) GR also contains an M_r 55000 protein that is recognized by anti-tubulin antibodies in Western blotting experiments. This copurification of tubulin with GR occurs after washing the immunoaffinity column with high salt buffers (1 M NaCl), strengthening the contention of a specific GR-tubulin interaction.

It has recently been shown that another stress protein subfamily, i.e., hsp70, is involved in the transport of certain proteins to microsomes and mitochondria [9, 14], possibly by "unfolding" the proteins to be transported. Whether hsp90 plays a similar role in the transport of GR to the nucleus has yet to be investigated.

The functional significance of an interaction between GR and MTs is presently unclear. Considering the importance of MTs in cellular locomotion, transport and division, it will be of interest to analyze if GR directly affects such cellular functions. In contrast to several other steroid hormone receptors, GR has been demonstrated in both cytoplasm and nucleus [45], and one could speculate that MTs may serve as translocation tracks directing GR back and forth between these two compartments during GR-activation. One previous report has indicated that MT-inhibitory agents seem to influence intracellular GR-transport [27]. It was found that treatment with colchicine prior to adrenalectomy delays both depletion and replenishment of liver cytosolic binding sites for dexamethasone, as compared to nontreated animals. This finding was not influenced by cycloheximide. In another study, neither vinblastine nor cytochalasin B had any effect on the estrogen-induced nuclear affinity of the estrogen receptor (ER) in rat uterus [22]. In the light of later findings demonstrating that ER is mainly a nuclear protein [28, 29], this result is not surprising.

GR-translocation in vitro and in vivo is generally accepted to be temperature dependent. The translocation is reversibly inhibited at +4 °C, i.e., glucocorticoids bind irreversibly to GR but are unable to translocate to the nucleus [24, 26]. This could well fit with the fact that the cytoplasmic MTs are completely depolymerized and thereby non-functioning at this temperature [20]. Thus, it is not inconceivable that MTs might play a role in the intracellular transport and processing of GR.

Acknowledgements. The authors wish to thank Eva Bergdahl for valuable and encouraging technical assistance. We also thank Per-Erik Strömstedt for help with purification of GR. Margareta Wallin's gift of purified calf brain tubulin is greatly appreciated. — This work was supported by grants from the Swedish Medical Research Council (no. 13X-2819) and from the Swedish Cancer Society (no. 1940). — Ann-Charlotte Wikström is a recipient of a fellowship from the Swedish Medical Research Council.

References

[1] Antakly, T., H. J. Eisen: Immunocytochemical localization of glucocorticoid receptor in target cells. Endocrinology **115**, 1984–1989 (1984).

[2] Aronow, L.: Effects of glucocorticoids on fibroblasts. In: J. D. Baxter, G. G. Rousseau (eds.): Glucocorticoid Hormone Action. Monographs on Endocrinology. pp. 327–340. Springer-Verlag. Berlin, Heidelberg 1979.

[3] Bernard, P. A., T. H. Joh: Characterization and immunocytochemical demonstration of glucocorticoid receptor using antisera specific to transformed receptor. Arch. Biochem. Biophys. **229**, 466–476 (1984).

[4] Bhisey, A. N., J. J. Freed: Ameboid movement induced in cultured macrophages by colchicine or vinblastine. Exp. Cell Res. **64**, 419–429 (1971).

[5] Borisy, G. G., J. B. Olmsted, J. M. Marcum, C. Allen: Microtubule assembly in vitro. Fed. Proc. Am. Soc. Exp. Biol. **33**, 167–174 (1974).

[6] Bradford, M. M.: A rapid and sensitive method for the quantitation of microgram quantities of protein utilizing the principle of protein-dye binding. Anal. Biochem. **72**, 248–254 (1976).

[7] Bruning, P. F., W. J. Meyer, C. M. Migeon: Glucocorticoid receptor in cultured human skin fibroblasts. J. Steroid Biochem. **10**, 587–593 (1979).

[8] Brönnegård, M., L. Poellinger, S. Okret, A.-C. Wikström, O. Bakke, J.-Å. Gustafsson: Characterization and sequence-specific binding to mouse mammary tumor virus DNA of purified activated human glucocorticoid receptor. Biochemistry **26**, 1697–1704 (1987).

[9] Chirico, W. J., M. W. Waters, G. Blobel: 70K heat shock related proteins stimulate protein translocation into microsomes. Nature **332**, 805–810 (1988).

[10] De Brabander, M., J. De Mey, G. Geuens, R. Nuydens, F. Aerts, R. Willebrords, M. Moeremans: Microtubules in cell organization and motility. In: J. E. Dumont, B. Hamprecht, J. Nuñez (eds.): Hormones and Cell Regulation. INSERM European Symposium. Vol. 9. pp. 85–104. Elsevier Science Publishers BV. Amsterdam 1985.

[11] Denis, M., A.-C. Wikström, J.-Å. Gustafsson: The molybdate-stabilized nonactivated glucocorticoid receptor contains a dimer of M_r 90000 non-hormone-binding protein. J. Biol. Chem. **262**, 11803–11806 (1987).

[12] Denis, M., L. Poellinger, A.-C. Wikström, J.-Å. Gustafsson: Requirement of hormone for thermal conversion of the glucocorticoid receptor to a DNA-binding state. Nature **333**, 686–688 (1988).

[13] Denis, M., J.-Å. Gustafsson, A.-C. Wikström: Interaction of the M_r 90000 heat shock protein with the steroid binding domain of the glucocorticoid receptor. J. Biol. Chem. **263**, 18520-18523 (1988).

[14] Deshaies, R. J., B. D. Koch, M. Werner-Washburne, E. A. Craig, R. Schekman: A subfamily of stress proteins facilitates translocation of secretory and mitochondrial precursor polypeptides. Nature **332,** 800–805 (1988).
[15] Erickson, H. P.: The structure and assembly of microtubules. Ann. NY Acad. Sci. **253,** 60–77 (1975).
[16] Fujiwara, K., L. G. Tilney: Substructural analysis of the microtubule and its polymorphic forms. Ann. NY Acad. Sci. **253,** 27–50 (1975).
[17] Fuxe, K., A.-C. Wikström, S. Okret, L. F. Agnati, A. Härfstrand, Z.-Y. Yu, L. Granholm, M. Zoli, W. Vale, J.-Å. Gustafsson: Mapping of glucocorticoid receptor immunoreactive neurons in the rat tel- and diencephalon using a monoclonal antibody against rat liver glucocorticoid receptor. Endocrinology **117,** 1803–1812 (1985).
[18] Gadson, P. F., J. D. Russell, S. B. Russell: Glucocorticoid receptors in human fibroblasts derived from normal dermis and keloid tissue. J. Biol. Chem. **18,** 11236–11241 (1984).
[19] Gasc, J.-M., E. E. Baulieu: Steroid hormone receptors: intracellular distribution. Biol. Cell **56,** 1–6 (1986).
[20] Gaskin, F., C. R. Cantor, M. L. Shelanski: Biochemical studies on the in vitro assembly and disassembly of microtubules. Ann. NY Acad. Sci. **253,** 133–146 (1975).
[21] Goldman, R. D., G. Berg, A. Bushnell, C.-M. Chang, L. Dickerman, N. Hopkins, M. L. Miller, R. Pollack, E. Wang: Fibrillar systems in cell motility. In: R. Porter, D. Fitz Simons (eds.): Ciba Foundation Symposium 14 (new series): Locomotion of tissue cells. pp 94–98. Elsevier. Amsterdam 1973.
[22] Gorski, J., B. Raker: The effects of cytochalasin B on estrogen binding and 2-deoxyglucose metabolism in the rat uterus. Endocrinology **93,** 1212–1216 (1973).
[23] Govindan, M. V.: Immunofluorescence microscopy of the intracellular translocation of glucocorticoid receptor complexes in rat hepatoma (HTC) cells. Exp. Cell Res. **127,** 293–297 (1980).
[24] Gustafsson, J.-Å., J. Carlstedt-Duke, L. Poellinger, S. Okret, A.-C. Wikström, M. Brönnegård, M. Gillner, Y. Dong, K. Fuxe, A. Cintra, A. Härfstrand, L. Agnati: Biochemistry, molecular biology, and physiology of the glucocorticoid receptor. Endocr. Rev. **8,** 185–234 (1987).
[25] Heuser, J. E., M. W. Kirschner: Filament organization revealed in platinum replicas of freeze-dried cytoskeletons. J. Cell Biol. **86,** 212–234 (1980).
[26] Ishii, D. N., W. B. Pratt, L. Aronow: Steady state level of the specific glucocorticoid binding component in mouse fibroblasts. Biochemistry **11,** 3896–3904 (1972).
[27] Ichii, S., A. Yoshida: Effect of colchicine on the depletion and replenishment of cytoplasmic glucocorticoid receptor in rat liver after administration of glucocorticoid. Endocrinol. Japon. **32,** 225–231 (1985).
[28] Jensen, E. V., T. Suzuki, T. Kawashima, W. E. Stumpf, P. W. Jungblut, E. R. De Sombre: A two-step mechanism for the interaction of estradiol with rat uterus. Proc. Natl. Acad. Sci. USA **59,** 632–638 (1968).
[29] King, W. J., G. L. Greene: Monoclonal antibodies localize estrogen receptor in the nuclei of target cells. Nature **307,** 745–747 (1984).
[30] Koyasu, S., E. Nishida, T. Kadowaki, F. Matsuzaki, K. Iida, F. Harada, M. Kasuga, H. Sakai, I. Yahara: Two mammalian heat shock proteins, hsp90 and hsp100, are actin binding proteins. Proc. Natl. Acad. Sci. USA **83,** 8054–8058 (1986).
[31] Koyasu, S., E. Nishida, Y. Miyata, H. Sakai, I. Yahara: Hsp100, a 100-kDa heat shock protein, is a Ca^{2+}-calmodulin-regulated actin-binding protein. J. Biol. Chem. **264,** 15083–15087 (1989).
[32] Laemmli, U. K.: Cleavage of structural proteins during the assembly of the head of bacteriophage T4. Nature **227,** 680–685 (1970).
[33] Lazarides, E., K. Weber: Actin antibody: the specific visualization of actin filaments in non-muscle cells. Proc. Natl. Acad. Sci. USA **6,** 2268–2272 (1974).
[34] Munck, A., K. Leung: Glucocorticoid receptors and mechanisms of action. In: J. R. Pasqualini (ed.): Receptors and Mechanisms of Action of Steroid Hormones. Part 2. pp. 311–397. Marcel Dekker. New York 1977.
[35] Okret, S., A.-C. Wikström, Ö. Wrange, B. Andersson, J.-Å. Gustafsson: Monoclonal antibodies against the rat liver glucocorticoid receptor. Proc. Natl. Acad. Sci. USA **81,** 1609–1613 (1984).
[36] Papamichail, M., G. Tsokos, N. Tsawdaroglou, C. E. Sekeris: Immunocytochemical demonstration of glucocorticoid receptors in different cell types and their translocation from the cytoplasm to the cell nucleus in the presence of dexamethasone. Exp. Cell Res. **125,** 490–493 (1980).
[37] Picard, D., K. R. Yamamoto: Two signals mediate hormone-dependent nuclear localization of the glucocorticoid receptor. EMBO J. **11,** 3333–3340 (1987).
[38] Pratt, W. B.: Transformation of glucocorticoid and progesterone receptors to the DNA-binding state. J. Cell. Biochem. **35,** 51–68 (1987).
[39] Pratt, W. B., E. R. Sanchez, E. H. Bresnick, S. Meshinchi, L. C. Scherrer, F. C. Dalman, M. J. Welsh: Interaction of the glucocorticoid receptor with the M_r 90000 heat shock protein: an evolving model of ligand-mediated receptor transformation and translocation. Cancer Res. **15;** 49 (8 Suppl.) 2222 s–2229 s (1989).
[40] Redmond, T., E. R. Sanchez, E. H. Bresnick, M. J. Schlesinger, D. O. Toft, W. B. Pratt, M. J. Welsh: Immunofluorescence colocalization of the 90-kDa heat-shock protein and microtubules in interphase and mitotic mammalian cells. Eur. J. Cell Biol. **50,** 66–75 (1989).
[41] Robertson, N. M., W. F. Kusmik, B. F. Grove, A. Miller-Diener, M. L. Webb, G. Litwack: Characterization of a monoclonal antibody that probes the functional domains of the glucocorticoid receptor. Biochem. J. **246,** 55–65 (1987).
[42] Titus, J. A., R. Haugland, S. O. Sharrow, D. M. Segal: Texas red, a hydrophilic, red-emitting fluorophore for use with fluorescein in dual parameter flow microfluorometric and fluorescence microscopic studies. J. Immunol. Methods **50,** 193–204 (1982).
[43] Weber, K., R. Pollack, T. Bibring: Antibody against tubulin: the specific visualization of cytoplasmic microtubules in tissue culture cells. Proc. Natl. Acad. Sci. USA **2,** 459–463 (1975).
[44] Weber, K., M. Osborn: Microtubule and intermediate filament networks in cells viewed by immunofluorescence microscopy. In: G. Poste, G. L. Nicolson (eds.): Cytoskeletal Elements and Plasma Membrane Organization. Vol. 7. Cell Surface Reviews. pp. 1–53. North Holland Publ. Co. Amsterdam 1981.
[45] Wikström, A.-C., O. Bakke, S. Okret, M. Brönnegård, J.-Å. Gustafsson: Intracellular localization of the glucocorticoid receptor: evidence for cytoplasmic and nuclear localization. Endocrinology **120,** 1232–1242 (1987).
[46] Willingham, M. C., I. Pastan: An Atlas of Immunofluorescence in Cultured Cells. pp. 152–173. Academic Press. Inc. Orlando, FL 1985.
[47] Wrange, Ö., J. Carlstedt-Duke, J.-Å. Gustafsson: Purification of glucocorticoid receptor from rat liver cytosol. J. Biol. Chem. **254,** 9284–9290 (1979).
[48] Yamamoto, K. R.: Steroid receptor regulated transcription of specific genes and gene networks. Annu. Rev. Gen. **19,** 209–252 (1985).